Available online at www.sciencedirect.com
SCIENCE DIRECT®
International Journal of Heat and Mass Transfer 49 (2006) 2619–2625
International Journal of HEAT and MASS TRANSFER
www.elsevier.com/locate/ijhmt

Fin spacing optimization of a fin-tube heat exchanger under frosting conditions

Dong-Keun Yang [1], Kwan-Soo Lee *, Simon Song

School of Mechanical Engineering, Hanyang University, 17 Haengdang-dong, Sungdong-gu, Seoul 133-791, Republic of Korea

Received 31 August 2005; received in revised form 9 January 2006
Available online 22 March 2006

Abstract

Optimal values of the design parameters for a fin-tube heat exchanger of a household refrigerator under frosting conditions are proposed to improve its thermal performance and extend its operating time. In the optimization procedure, fin spacings of the heat exchanger are selected as the design parameters, and the average heat transfer rate, frost mass, and operating time are considered to be objective functions. The response surface and Taguchi methods are employed to optimize the design parameters. As a result, the average heat transfer rate and operating time of the optimum models increases by up to 6.3% and 12.9% compared to that of the reference model, respectively.

Keywords: Optimization; Fin-tube heat exchanger; Frosting conditions

1. Introduction

In industrial or domestic refrigerator and air-conditioning systems, system efficiency is an important factor that attracts customers, especially in this era of high gas prices. A more efficient system provides better thermal performance reducing operating costs. One of most important factors that affect the thermal performance of a heat exchanger is frost formation on its surfaces. However, the thermal performance of a heat exchanger operating under frosting conditions has been evaluated experimentally in most cases, and the design parameters such as the fin spacing have been determined empirically. In order to improve the performance of a heat exchanger under frosting conditions, an optimization of the heat exchanger design should be considered.

In order to optimize a heat exchanger, an accurate model for predicting its frosting behavior must be developed. Frost formation phenomena on a cold plate and cylinder under various operating conditions have been examined both experimentally [1–6] and numerically [7–17]. However, most heat exchangers used in industrial and domestic refrigerators have been developed experimentally [18–20]. As a result, there are few analytic studies for frosting behavior of real heat exchangers [21–25]. Therefore, repeated experiments are required using many prototypes under various conditions to predict the frosting behavior of a given heat exchanger, resulting in a high development cost. Recently, optimization techniques have been applied frequently in the development of thermal systems, but few studies that have used these techniques for heat exchangers under frosting conditions have been reported in the literature.

This paper addresses the optimization of a heat exchanger under frosting conditions using the response surface and Taguchi methods. A mathematical model developed by our group [26] is adapted to predict the frosting behavior on a fin-tube heat exchanger.

* Corresponding author. Tel.: +82 2 2220 0426; fax: +82 2 2295 9021. *E-mail address:* ksleehy@hanyang.ac.kr (K.-S. Lee).
[1] Present address: Digital Appliance Research Laboratory, LG Electronics Inc., 222-22 Guro3-dong, Guro-gu, Seoul 152-848, Republic of Korea.

0017-9310/$ - see front matter © 2006 Elsevier Ltd. All rights reserved.
doi:10.1016/j.ijheatmasstransfer.2006.01.016

Nomenclature

A–F	design parameters for the Taguchi method
f	objective function
m_f	frost mass (g)
n	number of design points
P_{f2}–P_{f7}	fin spacing (mm)
Q_{ave}	average heat transfer rate (W)
T	temperature (K)
t_{op}	operating time (min)
u_a	air velocity (m/s)
w_a	absolute humidity (kg/kg$_a$)
w_1–w_2	weighting factors
X_i	normalized design parameters

Greek symbols

β	response surface coefficient
η	objective function variation rate

Subscripts

a	air
r	refrigerant
ref	reference

2. Frost modeling

Before optimizing the design parameters of a heat exchanger under frosting condition, it is required to predict the frosting behavior. In the present study, we use a mathematical model [26] that predicts thermal performance of a fin-tube heat exchanger under frosting conditions. For simplicity, the essence of the model is briefly introduced below.

The model consists of two parts of heat and mass transfer analysis: one between the air and the fin and tube of a heat exchanger, and the other inside the frost layer. To calculate the heat transfer rates between the air and the fin and tube, correlations for heat transfer coefficient (Eqs. (27) and (28) in Ref. [26]) experimentally obtained between the air and the cold flat plate and circular cylinder was used. The heat and mass transfer rates were separately calculated between the air and the fin and between the air and the tube. To predict the frosting behavior, the model utilizes a water-vapor diffusion equation (Eq. (15) in Ref. [26]) and correlations for the effective thermal conductivity of the frost layer (Eqs. (8)–(10) in Ref. [26]). The two analyses were coupled to reflect growth of the frost layer and the resulting surface temperature variation of the fin and tube.

To apply this model, a heat exchanger is divided into three-dimensional infinitesimal control volumes. The frosting behavior on each infinitesimal control volume is analyzed by considering the heat and mass balances simultaneously. The model was validated by comparing numerical results with experimental data for the frost thickness, frost mass, and heat transfer rate on simple and typical fin-tube heat exchangers. In the current study, this model was used to predict the frosting behavior of heat exchanger.

3. Optimum design problem definition

An optimum design problem may be defined by considering objective functions and constraint conditions. For the current study, the frost mass, average heat transfer rate, and operating time that affect the frosting and defrosting performances were selected as the objective functions. The permissible ranges of fin spacing were used as constraint conditions. Using the response surface [27] and Taguchi methods [28], the fin-spacing values were optimized to improve the performance of the heat exchanger.

The reference heat exchanger used in the current study is shown in Fig. 1, and its geometric parameters are listed in Table 1. The heat exchanger has 2 columns and 8 rows, and numerous fins are attached to the tube in each row. The fin-spacing values of the first and the eighth rows are fixed as 20 mm and 5 mm, respectively, due to the given design restrictions. The fin-spacing values of rows 2–7 (P_{f2}, P_{f3}, P_{f4}, P_{f5}, P_{f6}, P_{f7}) were allowed to vary and were selected as the design parameters. The upper and lower limits of the permissible spacing values are the constraint conditions that are determined considering the values of the reference

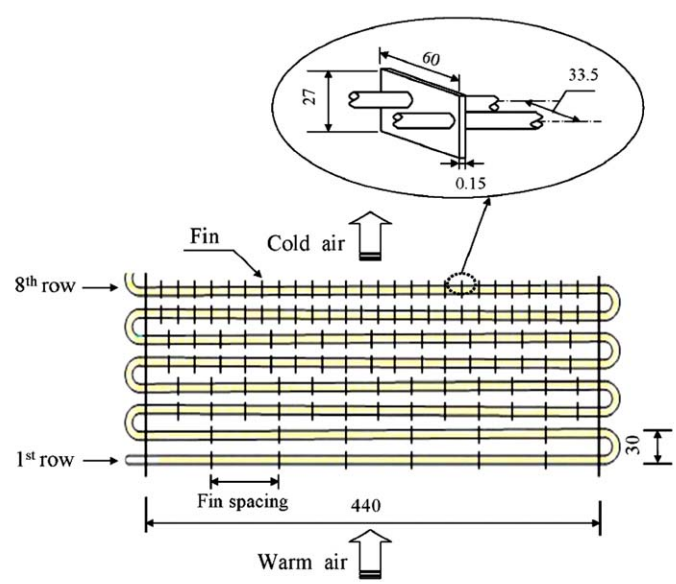

Fig. 1. Schematic diagram of a general fin-tube heat exchanger. The close look shows the dimensions (mm) of fin width, length and thickness and the tube spacing between the two columns.

Table 1
Geometric parameters of a typical fin-tube heat exchanger

Parameters	Values
Fin width	60 mm
Fin length	27 mm
Fin thickness	0.15 mm
Fin spacing	
Row 1,2	20 mm
Row 3,4	10 mm
Row 5.6	7.5 mm
Row 7,8	5 mm
Number of columns	2
Number of rows	8
Tube length	440 mm
Outer tube diameter	8.5 mm
Transverse tube spacing	25 mm
Longitudinal tube spacing	30 mm

heat exchanger as follows. Note that the constraint conditions are applied to both columns of the heat exchanger

$$\begin{aligned} &10\text{ mm} \leqslant P_{f2} \leqslant 20\text{ mm}, \quad 7.5\text{ mm} \leqslant P_{f3} \leqslant 12.5\text{ mm} \\ &7.5\text{ mm} \leqslant P_{f4} \leqslant 12.5\text{ mm}, \quad 5\text{ mm} \leqslant P_{f5} \leqslant 10\text{ mm} \\ &5\text{ mm} \leqslant P_{f6} \leqslant 10\text{ mm}, \quad 5\text{ mm} \leqslant P_{f7} \leqslant 10\text{ mm} \end{aligned} \tag{1}$$

The objective function for optimizing the design parameters was defined by

$$f(P_{f2}, P_{f3}, P_{f4}, P_{f5}, P_{f6}, P_{f7}) = w_1 \frac{Q_{ave}}{Q_{ave,ref}} + (1 - w_1) \frac{m_{f,ref}}{m_f} \tag{2}$$

where w_1 represents a weighting factor for the average heat transfer rate. When $w_1 = 1$, the system is optimized only for the average heat transfer rate.

4. Response surface method

The design parameters were optimized using the response surface method. As a first step, the design parameters (P_{f2}, P_{f3}, P_{f4}, P_{f5}, P_{f6}, P_{f7}) were normalized considering the upper ($P_{fi,max}$) and lower ($P_{fi,min}$) limits of the constraint conditions of each parameter as follows:

$$X_i = \frac{2(P_{fi} - P_{f,ref})}{P_{fi,max} - P_{fi,min}} \tag{3}$$

The normalized parameters (X_1, X_2, X_3, X_4, X_5, X_6) including the reference values ($P_{f,ref}$) are listed in Table 2. Various response surfaces may be generated using different weighting factors corresponding to the objective function of Eq. (2). The general form of the response surfaces for the objective function is given as

$$f(X_1, X_2, \ldots, X_n) = \beta_0 + \sum_{i=1}^{n} \beta_i X_i + \sum_{i=1}^{n} \beta_{ii} X_i^2 + \sum_{i<j}^{n} \beta_{ij} X_i X_j \tag{4}$$

Using the objective function and constraint conditions, an optimum design problem is defined as follows:

$$\begin{aligned} &\text{Max} \quad f(X_1, X_2, \ldots, X_6) \\ &\text{s.t.} \quad -1 \leqslant X_i \leqslant 1, \quad i = 1, 6 \end{aligned} \tag{5}$$

Table 2
Ranges and levels of normalized design parameters in the design of experiment

Design parameters	Ranges and levels		
	−1	0 (reference value)	1
$X_1(P_{f2})$	10.00 mm	15.00 mm	20.00 mm
$X_2(P_{f3})$	7.50 mm	10.00 mm	12.50 mm
$X_3(P_{f4})$	7.50 mm	10.00 mm	12.50 mm
$X_4(P_{f5})$	5.00 mm	7.50 mm	10.00 mm
$X_5(P_{f6})$	5.00 mm	7.50 mm	10.00 mm
$X_6(P_{f7})$	5.00 mm	7.50 mm	10.00 mm

4.1. Generation of the response surface

In order to generate a quadratic response surface using a central composite design, 77 design points consisting of the normalized design parameters were selected. Numerical analyses were performed at the design points using the frosting model [26]. The model assumed the use of R134a refrigerant and the following operating conditions: $T_r = -30$ °C, $u_a = 1.5$ m/s, $T_a = -11.1$ °C, and $w_a = 0.00145$ kg/kg$_a$. The operating time of the refrigerator was set to 390 min that is a typical defrosting period of industrial refrigerators.

Several response surfaces were obtained from the numerical analyses using various weighting factors and Eqs. (2) and (4). An analysis of variance (ANOVA) of the numerical results was performed to validate the accuracy of the various response surfaces. For example, the coefficient of determination for the response surface with $w_1 = 1.0$ was 0.985. The results demonstrated that the response surfaces accurately represent the relations between the design parameters and objective functions.

4.2. Optimum values

An optimum design problem may have several optimum values depending on the weighting factor, as shown in Table 3. Since the average heat transfer rate is more important than the frost mass in the design of a heat exchanger, the design parameters were only optimized for $w_1 \geqslant 0.5$. In the table, $\eta_{Q_{ave}}$ and η_{m_f} give the percentage increase of the average heat transfer rate and frost mass in the optimum model compared to the reference model. The optimum design that maximizes the average heat transfer rate of the heat exchanger was obtained when the normalized design parameters were $X_1 = -1$, $X_2 = -1$, $X_3 = -1$, $X_4 = -0.136$, $X_5 = -0.930$, and $X_6 = -1$ ($P_{f2} = 10.00$ mm, $P_{f3} = 7.50$ mm, $P_{f4} = 7.50$ mm, $P_{f5} = 7.16$ mm, $P_{f6} = 5.18$ mm, and $P_{f7} = 5.00$ mm). The average heat transfer rate in the optimum model increased by up to 6.3% compared to the reference model. One may select any optimum design shown in Table 3 based on the importance of each objective function.

Table 3
Optimum values for the design parameters using a response surface with weighting factors

Weighting factor (w_1)	X_1	X_2	X_3	X_4	X_5	X_6	f	$\eta_{Q_{ave}}$ (%)	η_{m_f} (%)
1.0	−1	−1	−1	−0.136	−0.930	−1	1.063	6.3	8.1
0.7	−1	−1	−1	−1	−1	−1	1.025	4.3	1.9
0.5	1	0.255	0.243	−1	−1	−1	1.031	−0.9	−6.6

5. Taguchi method

The Taguchi method is efficient for a design problem with several parameters and is frequently used in industry because it can readily improve a reference model based on the objective function without repeating experiments. For example, the computational effort required for the Taguchi method increases little when the number of design parameters increases unlike the response surface method. Also, the Taguchi method is superior in applying an optimum design to real products because it proposes an optimum model based on a combination of feasible design parameters. Thus, the Taguchi method is especially effective for improving the design of products that have already been manufactured.

5.1. Optimization

The Taguchi optimization procedure adapted for the current study is as follows. First, the value of each design parameter used for the response surface method was divided into three levels, as shown in Table 4. The design parameters (P_{f2}, P_{f3}, P_{f4}, P_{f5}, P_{f6}, P_{f7}) were renamed as A, B, C, D, E, and F for convenience. Since all selected design parameters had a similar influence on the objective function, they were all divided into the same three levels. Numerical analyses were performed to optimize the performance of the heat exchanger using the $L_{27}(3^6)$ orthogonal array table for the design points shown in Table 5 and the objective function given by Eq. (2). Table 6 shows the signal-to-noise (S/N) ratio defined by the Taguchi method.

Fig. 2 shows the effects of the design parameters on the S/N ratios for $w_1 = 1.0$. The optimum values of the design parameters correspond to the design point that has the maximum S/N ratio. According to Fig. 2, the optimum levels of the design parameters when $w_1 = 1.0$ were $A_1B_1C_1D_2E_2F_1$. Table 7 summarizes the optimum levels of the design parameters for the three weighting factors, and provides the percentage increase of the frost mass and average heat transfer rate of the optimum models compared to the reference model. For example, the average heat transfer rate improved by 5.5% in the optimum model with $w_1 = 1.0$. The optimum models provided either a higher average heat transfer rate or a lower frost mass, depending on the weighting factor.

Table 4
Design parameters of a three-level Taguchi method

Design parameters	Level		
	1	2	3
$A(P_{f2})$	10.00 mm	15.00 mm	20.00 mm
$B(P_{f3})$	7.50 mm	10.00 mm	12.50 mm
$C(P_{f4})$	7.50 mm	10.00 mm	12.50 mm
$D(P_{f5})$	5.00 mm	7.50 mm	10.00 mm
$E(P_{f6})$	5.00 mm	7.50 mm	10.00 mm
$F(P_{f7})$	5.00 mm	7.50 mm	10.00 mm

5.2. Optimization for operating time

The performance of the heat exchanger under frosting conditions can be augmented not only by improving its thermal performance but also by increasing its operating time. In this section, results of the heat exchanger optimization to extend its operating time are reported using the Taguchi method. Note that the objective function of Eq. (2) is composed of the average heat transfer rate and frost mass. Thus, another objective function should be defined using the operating time and average heat transfer rate as follows:

Table 5
$L_{27}(3^6)$ orthogonal array table for the Taguchi method

Test number	Design parameters					
	A	B	C	D	E	F
1	1	1	1	1	1	1
2	1	1	1	1	2	2
3	1	1	1	1	3	3
4	1	2	2	2	1	1
5	1	2	2	2	2	2
6	1	2	2	2	3	3
7	1	3	3	3	1	1
8	1	3	3	3	2	2
9	1	3	3	3	3	3
10	2	1	2	3	1	2
11	2	1	2	3	2	3
12	2	1	2	3	3	1
13	2	2	3	1	1	2
14	2	2	3	1	2	3
15	2	2	3	1	3	1
16	2	3	1	2	1	2
17	2	3	1	2	2	3
18	2	3	1	2	3	1
19	3	1	3	2	1	3
20	3	1	3	2	2	1
21	3	1	3	2	3	2
22	3	2	1	3	1	3
23	3	2	1	3	2	1
24	3	2	1	3	3	2
25	3	3	2	1	1	3
26	3	3	2	1	2	1
27	3	3	2	1	3	2

Table 6
S/N ratio for the Taguchi method

Characteristics	S/N ratio
Smaller-the-better	$-10\log\left[\frac{1}{n}\sum_{i=1}^{n} f_i^2\right]$
Larger-the-better	$-10\log\left[\frac{1}{n}\sum_{i=1}^{n} \frac{1}{f_i^2}\right]$

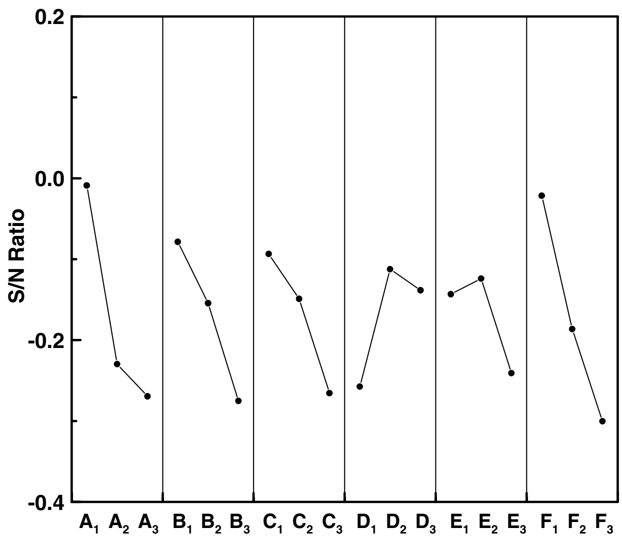

Fig. 2. Effects of the design parameters on the S/N ratios for $w_1 = 1.0$.

$$f(A,B,C,D,E,F) = w_2\frac{t_{op}}{t_{op,ref}} + (1-w_2)\frac{Q_{ave}}{Q_{ave,ref}} \quad (6)$$

where w_2 and $t_{op,ref}$ represent the weighting factor for the operating time and reference operating time, respectively. Also, t_{op} indicates the operating time at which the airflow blockage ratio of the heat exchanger becomes the same as the ratio of the reference heat exchanger at $t = 390$ min.

Table 8 lists the optimum designs for the heat exchanger with respect to Eq. (6) and five weighting factors. In the table, $\eta_{t_{op}}$ gives the percentage increase of the operating times for the optimum model compared to the reference model. The operating time of the optimum model increased by up to 12.9% without a decrease in the average heat transfer rate.

5.3. Effects of operating conditions

The operating conditions for the heat exchanger, such as the refrigerant temperature, air velocity, air humidity, and air temperature, can vary with the user characteristics and surrounding environment. Thus, optimizations using the objective function given by Eq. (2) with $w_1 = 1.0$ were also performed for the following operating conditions:

Reference case: $u_a = 1.5$ m/s, $T_a = -11.1$ °C, $w_a = 0.00145$ kg/kg$_a$, $T_r = -30$ °C.
Case 1: $u_a = 1.2$ m/s, $T_a = -11.1$ °C, $w_a = 0.00145$ kg/kg$_a$, $T_r = -30$ °C.
Case 2: $u_a = 1.8$ m/s, $T_a = -11.1$ °C, $w_a = 0.00145$ kg/kg$_a$, $T_r = -30$ °C.
Case 3: $u_a = 1.5$ m/s, $T_a = -11.1$ °C, $w_a = 0.00145$ kg/kg$_a$, $T_r = -27$ °C.
Case 4: $u_a = 1.5$ m/s, $T_a = -11.1$ °C, $w_a = 0.00145$ kg/kg$_a$, $T_r = -33$ °C.
Case 5: $u_a = 1.5$ m/s, $T_a = -13.4$ °C, $w_a = 0.00118$ kg/kg$_a$, $T_r = -30$ °C.
Case 6: $u_a = 1.5$ m/s, $T_a = -8.8$ °C, $w_a = 0.00178$ kg/kg$_a$, $T_r = -30$ °C.

Table 9 shows the optimum values of three-level design parameters for the above six cases. The fin spacings in the optimum model decreased with increasing refrigerant temperature and decreasing air temperature to compensate for

Table 7
Optimum values for the three-level design parameters using the Taguchi method with weighting factors

Weighting factor (w_1)	A	B	C	D	E	F	f	$\eta_{Q_{ave}}$ (%)	η_{m_f} (%)
1.0	1	1	1	2	2	1	1.055	5.5	8.5
0.7	1	1	1	1	1	1	1.025	4.3	1.9
0.5	3	3	3	1	1	1	1.032	−2.2	−7.8

Table 8
Optimum values for the three-level design parameters using the objective function (Eq. (6)) with weighting factors

Weighting factor (w_2)	A	B	C	D	E	F	f	$\eta_{t_{op}}$ (%)	$\eta_{Q_{ave}}$ (%)
1.0	1	2	1	2	2	2	1.129	12.9	0.1
0.7	1	2	1	2	2	2	1.091	12.9	0.1
0.5	1	2	1	2	2	2	1.065	12.9	0.1
0.3	1	1	1	2	2	1	1.040	2.2	4.8
0.0	1	1	1	1	1	1	1.100	−14.8	10.0

Table 9
Optimum values for the three-level design parameters using the objective function (Eq. (2)) for $w_1 = 1.0$ with operating conditions

Case	*A*	*B*	*C*	*D*	*E*	*F*	*f*	$\eta_{Q_{ave}}$ (%)	η_{m_f} (%)
Reference	1	1	1	2	2	1	1.055	5.5	8.5
1	1	1	1	2	2	1	1.057	5.7	5.9
2	1	1	1	2	2	1	1.055	5.5	5.2
3	1	1	1	2	1	1	1.059	5.9	4.3
4	1	1	1	2	2	1	1.054	5.4	7.7
5	1	1	1	2	1	1	1.062	6.2	7.4
6	1	1	1	2	2	1	1.054	5.4	3.4

the reduction in the heat transfer rate. However, differences of the optimum levels of the design parameters were minimal despite the variations in the operating conditions. Overall, the operating conditions had little effect on the optimum values of the design parameters.

6. Conclusions

This paper proposed optimal values of the design parameters for a fin-tube heat exchanger under operating conditions corresponding to those of a household freezer and refrigerator. An optimum design of the heat exchanger maximizing the average heat transfer rate was obtained using the response surface method. The average heat transfer rate of the optimum model increased by 6.3% compared to the reference model. When the heat exchanger was optimized using the Taguchi method, the average heat transfer rate increased by up to 5.5% compared to the reference model. An optimum model to extend the operating time was also proposed based on a Taguchi optimization. The operating time of this model increased by 12.9% compared to the reference operating time. Finally, the operating conditions had little effect on the choice of an optimum design for the heat exchanger.

Acknowledgement

This work was supported by the Center of Innovative Design Optimization Technology (iDOT), Korea Science and Engineering Foundation.

References

[1] H.W. Schneider, Equation of the growth rate of frost forming on cooled surfaces, Int. J. Heat Mass Transfer 21 (1978) 1019–1024.
[2] R. Östin, S. Anderson, Frost growth parameters in a forced air stream, Int. J. Heat Mass Transfer 14 (4–5) (1991) 1009–1017.
[3] J.D. Yonko, C.F. Sepsy, An investigation of the thermal conductivity of frost while forming on a flat horizontal plate, ASHRAE Trans. 73 (2) (1967) 1.1–1.11.
[4] Y. Mao, R.W. Besant, H. Chen, Frost characteristics and heat transfer on a flat plate under freezer operating conditions: Part 1, Experimentation and correlations, ASHRAE Trans. 105 (2) (1999) 231–251.
[5] Y. Hayashi, A. Aoki, S. Adachi, K. Hori, Study of frost properties correlation with frost formation types, ASME J. Heat Transfer 99 (1977) 239–245.
[6] D.K. Yang, K.S. Lee, Dimensionless correlations of frost properties on a cold plate, Int. J. Refrigeration 27 (1) (2004) 89–96.
[7] B.W. Jones, J.D. Parker, Frost formation with varying environmental parameters, J. Heat Transfer 97 (1975) 255–259.
[8] K.S. Lee, W.S. Kim, T.H. Lee, A one-dimensional model for frost formation on a cold flat surface, Int. J. Heat Mass Transfer 40 (18) (1997) 4359–4365.
[9] R. Yun, Y. Kim, M.K. Min, Modeling of frost growth and frost properties with airflow over a flat plate, Int. J. Refrigeration 25 (3) (2002) 362–371.
[10] K.S. Lee, S. Jhee, D.K. Yang, Prediction of the frost formation on a cold flat surface, Int. J. Heat Mass Transfer 46 (20) (2003) 3789–3796.
[11] P.J. Mago, S.A. Sherif, Heat and mass transfer on a cylinder surface in cross flow under supersaturated frosting conditions, Int. J. Refrigeration 26 (8) (2003) 889–899.
[12] S.P. Raju, S.A. Sherif, Frost formation and heat transfer on circular cylinders in cross-flow, Int. J. Refrigeration 16 (6) (1993) 390–401.
[13] K.A.R. Ismail, C.S. Salinas, Modeling of frost formation over parallel cold plates, Int. J. Refrigeration 22 (5) (1999) 425–441.
[14] R. LeGall, J.M. Grillot, C. Jallut, Modelling of frost growth and densification, Int. J. Heat Mass Transfer 40 (13) (1997) 3177–3187.
[15] H. Chen, R.W. Besant, Y.X. Tao, Frost characteristics and heat transfer on a flat plate under freezer operating conditions: Part II, Numerical modeling and comparison with data, ASHRAE Trans. 105 (1) (1999) 252–259.
[16] B. Na, R.L. Webb, New model for frost growth rate, Int. J. Heat Mass Transfer 47 (5) (2004) 925–936.
[17] D.K. Yang, K.S. Lee, D.J. Cha, Frost formation on a cold surface under turbulent flow, Int. J. Refrigeration 29 (2) (2006) 164–169.
[18] S. Jhee, K.S. Lee, W.S. Kim, Effect of surface treatments on the frosting/defrosting behavior of a fin-tube heat exchanger, Int. J. Refrigeration 25 (8) (2002) 1047–1053.
[19] W.M. Yan, H.Y. Li, Y.J. Wu, J.Y. Lin, W.R. Chang, Performance of finned tube heat exchangers operating under frosting conditions, Int. J. Heat Mass Transfer 46 (5) (2003) 871–877.
[20] D. Deng, L. Xu, S. Xu, Experimental investigation on the performance of air cooler under frosting conditions, Appl. Therm. Eng. 23 (8) (2003) 905–912.
[21] H. Yasuda, T. Senshu, S. Kuroda, A. Atsumi, K. Oguni, Heat pump performance under frosting conditions: Part II. Simulation of Heat pump cycle characteristics under frosting conditions, ASHRAE Trans. (1990) 330–336.
[22] S.N. Kondepudi, D.L. ON'eal, Performance of finned-tube heat exchangers under frosting conditions: I. Simulation model, Int. J. Refrigeration 16 (3) (1993) 175–180.
[23] S.N. Kondepudi, D.L. ON'eal, A simplified model of pin fin heat exchangers under frosting conditions, ASHRAE Trans. (1993) 754–761.
[24] Y. Yao, Y. Jiang, S. Deng, Z. Ma, A study on the performance of the airside heat exchanger under frosting in an air source heat pump water heater/chiller unit, Int. J. Heat Mass Transfer 47 (17–18) (2004) 3745–3756.

[25] D. Seker, H. Karatas, N. Egrican, Frost formation on fin-and-tube heat exchangers. Part I—Modeling of frost formation on fin-and-tube heat exchangers, Int. J. Refrigeration 27 (4) (2004) 367–374.
[26] D.K. Yang, K.S. Lee, S. Song, Modeling for predicting frosting behavior of a fin-tube heat exchanger, Int. J. Heat Mass Transfer 49 (7–8) (2006) 1472–1479.
[27] D.C. Montgomery, Design and Analysis of Experiments, John Wiley & Sons, Singapore, 1991.
[28] G. Taguchi, S. Chowdhury, S. Taguchi, Robust Engineering, McGraw-Hill, New York, 2000.